SUPPLEMENTARY MATERIAL

*Molecular Modeling of the TMX3 **abb'** Fragment*

As described in the "Experimental procedures" section we used the structures of human PDI **a** (1) and rabbit skeletal muscle calsequestrin (CSQrs) (2) as templates for the molecular modeling of TMX3 **abb'**. A priori, we could have used the crystal structure of either Pdi1p (3) or ERp57 **bb'** (4) instead of CSQrs for the modeling of the **bb'** region. However, the Pdi1p **bb'** sequence is not homologous to TMX3 **bb'**. While ERp57 **bb'** and CSQrs are equally similar to the TMX3 **bb'** sequence, the CSQrs structure holds the advantage of having an additional N-terminal thioredoxin domain that we here used to fix the domain orientation between the **a** and **b** domains. Moreover, the positions of secondary structure elements seem to be well conserved between CSQrs and TMX3 in the **bb'** region (Fig. S1), with the potential exception of the first β-strands in the **b** and **b'** domains in CSQrs that are not predicted for TMX3.

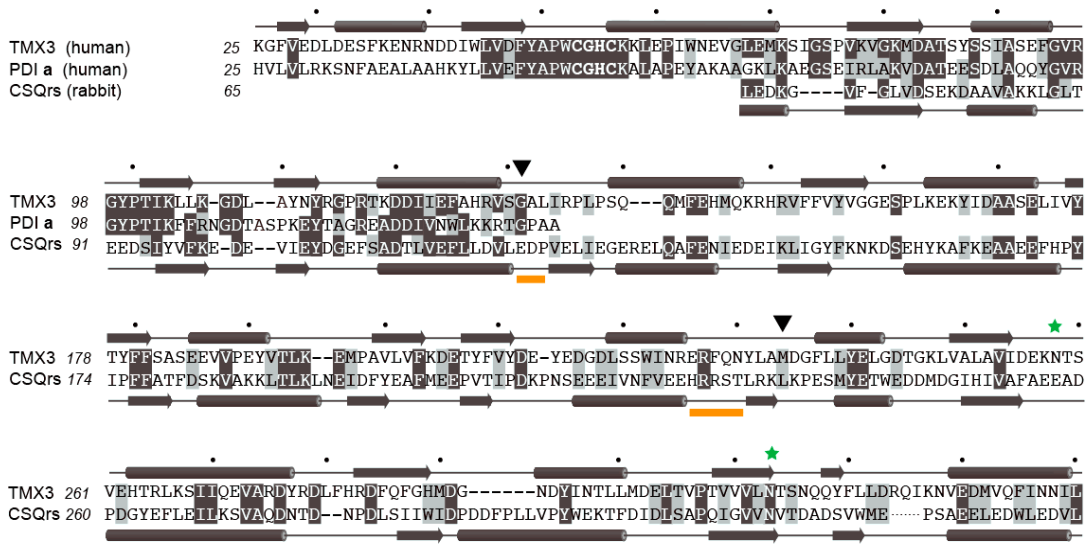

Fig. S1. Alignment used for modeling of the TMX3 **abb'** fragment comprising residues 25-340 of the native protein. The model is based on the NMR structure of human PDI **a** domain and the crystal structure of rabbit skeletal muscle calsequestrin (CSQrs). Only those residues from the template structures that were used for the modeling were included in the alignment (notice the overlap between the templates). In addition to the sequences, predicted secondary structure elements in TMX3 and experimentally determined secondary structure elements of the crystal structure of CSQrs are shown (helices and strands are represented by cylinders and arrows, respectively). The two orange bars below the CSQrs sequence show the positions of inter-domain linker regions. Green stars mark the positions of the two *N*-glycosylated residues in TMX3, Asn258 and Asn313. Black arrow heads point to the last residue in each of the TMX3 domain constructs, **a** and **ab** (residues G131 and M234, respectively). Three residues C-terminal of the last β-strand in CSQrs, a region of seven residues not observable in the electron density map were left out of the alignment (denoted by a row of dots). The dots above the sequence mark every tenth residue in TMX3.

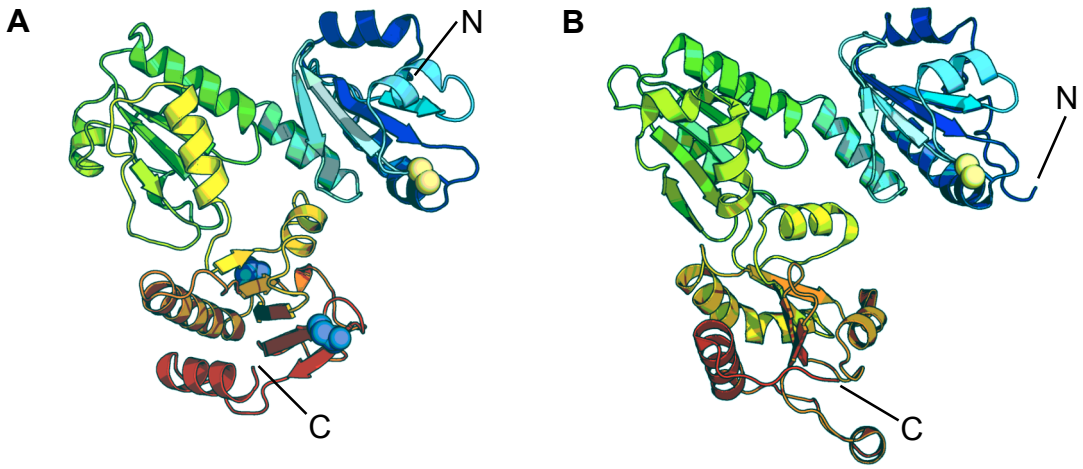

Fig. S2. Comparison of the TMX3 model with Pdi1p **abb'**. Both ribbon models are colored to emphasize the path of the polypeptide chain from blue at the N-terminus to red at the C-terminus via color changes to cyan, green, yellow and orange. The N- and C-termini are indicated. *A*, Model of TMX3 **abb'**. The active-site disulfide bridge in the CGHC motif is shown as yellow spheres, and the side-chain atoms of the two *N*-glycosylated residues Asn258 and Asn313 in the **b'** domain are shown as blue spheres. The domain orientations are based entirely on those of CSQ. *B*, The crystal structure of Pdi1p **abb'**.

Determination of the rate-limiting step in peptide oxidation

The rate-limiting step for the peptide oxidation reaction can be determined from analysis of the time-dependent fluorescence change, as it was recently done in a study comparing the reaction kinetics of a number of ER oxidoreductases (5). Two extreme cases give rise to two distinct reaction profiles – if peptide oxidation is rate limiting, the reaction behaves as a first-order reaction towards substrate resulting in an exponential decrease of the fluorescence signal, whereas an initial linear decrease of the signal is symptomatic for the case where enzyme reoxidation by GSSG is rate-limiting, and the reaction behaves as a zero-order reaction with respect to substrate (5). The reaction profiles from the experiments shown in Fig. 6*A-C* – performed at 500 µM GSSG – fit well to an exponential function with random residuals. Here, we used TMX3 **ab** and **abb'** to investigate details of the peptide oxidation reaction. Progressively lowering [GSSG] while maintaining $[GSSG]/[GSH]^2$ resulted in a decrease of the reaction rate of the uncatalyzed reaction proportional to the change of [GSSG], whereas the effect on the reaction rates of TMX3 **ab** and **abb'** was weaker. However, for reactions performed below a certain concentration of GSSG the decrease in fluorescence was linear for over 50% of the reaction (data not shown), indicating that reoxidation of the enzyme by GSSG became rate limiting. In a plot of the inverse half-times for the reaction *versus* [GSSG], a linear relation is observed over the concentration range where this is the case. As shown in Fig. S3, enzyme reoxidation was rate limiting until almost 250 µM GSSG for TMX3 **abb'**, whereas the corresponding concentration for TMX3 **ab** was significantly lower.

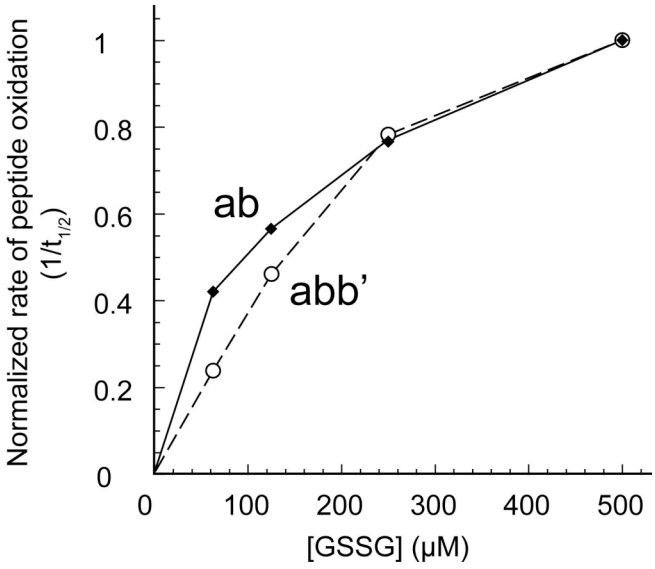

Fig. S3. Normalized inverse half-times of peptide oxidation by TMX3 **ab** (filled squares connected by straight solid lines) and TMX3 **abb'** (empty circles connected by straight dashed lines) in dependence of [GSSG]. The peptide oxidation assay was performed at four different concentrations of GSSG (63, 125, 250 and 500 µM). The inverse half-times of reaction were normalized to the values obtained at 500 µM GSSG for each construct and plotted *versus* the concentration of GSSG.

References

1. Kemmink, J., Darby, N. J., Dijkstra, K., Nilges, M., and Creighton, T. E. (1996) *Biochemistry* **35**, 7684-7691
2. Wang, S., Trumble, W. R., Liao, H., Wesson, C. R., Dunker, A. K., and Kang, C. H. (1998) *Nat. Struct. Biol.* **5**, 476-483
3. Tian, G., Xiang, S., Noiva, R., Lennarz, W. J., and Schindelin, H. (2006) *Cell* **124**, 61-73
4. Kozlov, G., Maattanen, P., Schrag, J. D., Pollock, S., Cygler, M., Nagar, B., Thomas, D. Y., and Gehring, K. (2006) *Structure* **14**, 1331-1339
5. Alanen, H. I., Salo, K. E., Pirneskoski, A., and Ruddock, L. W. (2006) *Antioxid. Redox. Signal.* **8**, 283-291